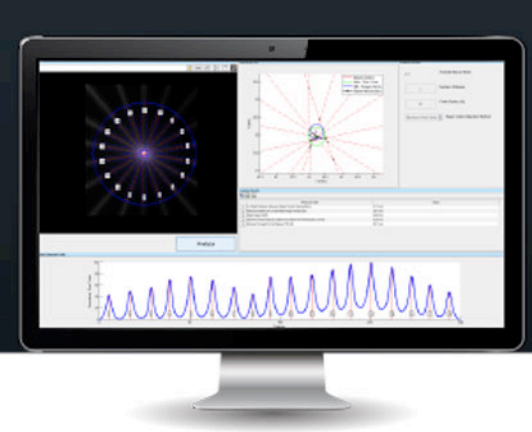

COMPREHENSIVE MACHINE QA SOLUTIONS

FROM RADIOLOGICAL IMAGING TECHNOLOGY, INC.

RIT software provides extensive machine QA capabilities, including comprehensive packages that can be used to perform a full suite of measurements in accordance with TG-142, TG-148, and/or TG-135. RIT's automated routines allow you to perform daily, monthly, and annual QA with efficiency, precision, and confidence knowing your delivery performance is optimized.

TG-142: LINEAR ACCELERATORS QA

RIT is the single-vendor software solution that performs and trends every test recommended in TG-142 and MPPG 8.a.

Perform comprehensive quality assurance of Varian, Elekta, and all linear accelerators with confidence and ease, using your EPID and RIT software. RIT *Complete*, RIT *Classic*, and RITG142 feature RIT's popular 3D Winston-Lutz Isocenter Optimization routine that will help your SRS/SBRT delivery with its sub-millimeter, fully-automated accuracy. RIT offers automated tests for Star Shot Analysis, Radiation vs. Light Field, MLC accuracy, and other beam measurements.

TG-148: HELICAL TOMOTHERAPY® QA

RIT offers a comprehensive test suite for helical TomoTherapy® and Radixact® machines, in accordance with TG-148.

Designed with the TG-148 report in mind, the RITG148+ and RIT *Complete* software packages analyze the standardized tests for helical TomoTherapy machine QA. These include Static & Rotational Output Consistency, Jaw Centering and Alignment, Overhead Laser Positioning, Interrupted Treatment, and all others recommended for daily, monthly, and annual QA. The software will also analyze image quality using the TomoTherapy Cheese phantom.

TG-135: CYBERKNIFE® ROBOTIC RADIOSURGERY QA

RIT provides a comprehensive test suite for CyberKnife® and all robotic radiosurgery, in accordance with TG-135.

The RITG135 and RIT *Complete* software packages contain five fully-automated QA tests for CyberKnife® machines: End-to-End Test, AQA Test, Iris Test, Laser Coincidence, and MLC (Garden Fence) Test for the M6 Collimator. Combining a user-friendly interface with automated film detection algorithms, the software eliminates the need for manual manipulation or alignment of images, and drastically reduces the time required to perform these tests.

RIT®

VISIT **RADIMAGE.COM** TO DEMO RIT'S ADVANCED RANGE OF MACHINE QA, MLC QA, PATIENT QA, AND IMAGING QA ROUTINES.

+1 (719) 590-1077, OPT. 4

SALES@RADIMAGE.COM

Visit us at the AAPM 2023 Annual Meeting in Houston, TX from July 23-26.
Exhibition Hall – Booth 621

Received: 13 January 2023 | Revised: 17 April 2023 | Accepted: 5 June 2023

DOI: 10.1002/mp.16564

RESEARCH ARTICLE

MEDICAL PHYSICS

Patient-specific quality assurance for deformable IMRT/IMPT dose accumulation: Proposition and validation of energy conservation based validation criterion

Xin Wu[1,2] | **Florian Amstutz**[1,3] | **Damien C. Weber**[1,4,5] | **Jan Unkelbach**[4] | **Antony J. Lomax**[1,3] | **Ye Zhang**[1]

[1]Center for Proton Therapy, Paul Scherrer Institute, Villigen, Switzerland

[2]Department of Information Technology & Electrical Engineering, ETH Zurich, Zurich, Switzerland

[3]Department of Physics, ETH Zurich, Zurich, Switzerland

[4]Department of Radiation Oncology, University Hospital Zurich, Zurich, Switzerland

[5]Department of Radiation Oncology, Inselspital, Bern University Hospital, University of Bern, Bern, Switzerland

Correspondence
Ye Zhang, Center for Proton Therapy, Forschungsstrasse 111, WMSA C27, 5232 Villigen PSI West, Switzerland
Email: ye.zhang@psi.ch

Funding information
The Swiss Cancer Research Foundation, Grant/Award Numbers: KFS-4528-08-2018, KFS-4517-08-2018

Abstract

Background: Deformable image registration (DIR)-based dose accumulation (DDA) is regularly used in adaptive radiotherapy research. However, the applicability and reliability of DDA for direct clinical usage are still being debated. One primary concern is the validity of DDA, particularly for scenarios with substantial anatomical changes, for which energy-conservation problems were observed in conceptual studies.

Purpose: We present and validate an energy-conservation (EC)-based DDA validation workflow and further investigate its usefulness for actual patient data, specifically for lung cancer cases.

Methods: For five non-small cell lung cancer (NSCLC) patients, DDA based on five selective DIR methods were calculated for five different treatment plans, which include one intensity-modulated photon therapy (IMRT), two intensity-modulated proton therapy (IMPT), and two combined proton-photon therapy (CPPT) plans. All plans were optimized on the planning CT (planCT) acquired in deep inspiration breath-hold (DIBH) and were re-optimized on the repeated DIBH CTs of three later fractions. The resulting fractional doses were warped back to the planCT using each DIR. An EC-based validation of the accumulation process was implemented and applied to all DDA results. Correlations between relative organ mass/volume variations and the extent of EC violation were then studied using Bayesian linear regression (BLR).

Results: For most OARs, EC violation within 10% is observed. However, for the PTVs and GTVs with substantial regression, severe overestimation of the fractional energy was found regardless of treatment type and applied DIR method. BLR results show that EC violation is linearly correlated to the relative mass variation ($R^2 > 0.95$) and volume variation ($R^2 > 0.60$).

Conclusion: DDA results should be used with caution in regions with high mass/volume variation for intensity-based DIRs. EC-based validation is a useful approach to provide patient-specific quality assurance of the validity of DDA in radiotherapy.

KEYWORDS
deformable image registration, Dose accumulation, lung cancer, photon therapy, proton therapy

Xin Wu and Florian Amstutz shared first authorship.

1 | INTRODUCTION

Adaptive radiation therapy (ART) showed to be able to deliver better target coverage and organ at risk (OAR) sparing for cancer patients undergoing anatomical changes,[1,2] for a number of cancers including but not limited to head and neck cancer,[3] prostate cancer,[4] and lung cancer.[5]

Deformable image registration (DIR) is one important component regularly used in ART workflow for contour propagation or dose warping based on the estimated correspondence between image pairs. The result of a DIR is a non-uniform deformation vector field (DVF) with three degrees of freedom for each voxel. Although, in theory, DIR should be able to deal with possible anatomical variation,[6] DIR itself is an ill-posed problem, lacking a ground truth solution.[7] Different DIRs algorithms have unavoidable discrepancies when registering the same input image pair.[8–10] Moreover, the results are sensitive to parameter choices even within one specific DIR algorithm.[11] As suggested by the AAPM task group 132,[12] validation and quality assurance (QA) of DIR is crucial, as these intrinsic discrepancies can be propagated to downstream applications of DIR, such as dose accumulation.

In ART, the fractional adaptation of the structures and treatment plans leads to non-trivial dose accumulation. For the presented work here, we assume that the doses of fractionated plans on varying anatomies need to be summed up to one reference anatomy, for example, the planning CT (planCT), such that the cumulative dose to the target and OARs can be evaluated.[13] Up to now, dose accumulation research is often based on DIR, therefore known as deformable dose accumulation (DDA).[14] A typical DDA workflow used in research is displayed in Figure 1 (brown box). First, new adaptive treatment plans are optimized for repeated CTs. The reference anatomy is registered with the repeated CTs using a DIR algorithm. Then, the re-optimized fraction dose distribution D_i is warped to the reference anatomy using the corresponding DVF ϕ for all fractions. Finally, the fraction doses are summed on the reference anatomy. Although DDA is an intuitive approach, multiple questions remain open, making clinical implementation challenging.[15] Different levels of uncertainties related to DDA are under investigation. On the application level, DIR ambiguities can propagate into dose accumulation, inducing uncertainty in the quantification of a confidence interval for DDA results. When applying multiple DIR algorithms, the underlying DDA uncertainties have been analyzed and shown to be substantial.[10] Additional research showed that these dosimetric uncertainties can be modeled and estimated with reasonable accuracy.[16] As DIR uncertainties are unavoidable, it is important to quantify these uncertainties before clinical decisions are taken. As a result, the clinical implementation of DIR should be done carefully, by exploring the limitation and applicability of the methods in different situations.[17,18]

In this work, we focus on a more general level by looking at the uncertainties of the DDA process itself. For most DIRs, the obtained DVFs are optimized by correlating the intensity similarity of the two input CT images. Therefore, it is questionable if image intensity correlations can directly be extrapolated to accumulate doses. In previous works, calculations performed on a deformable phantom with external force indeed showed that DDA has limited accuracy in regions with a higher magnitude of deformation.[19] Furthermore, large deformations appearing in regions with volume and/or mass

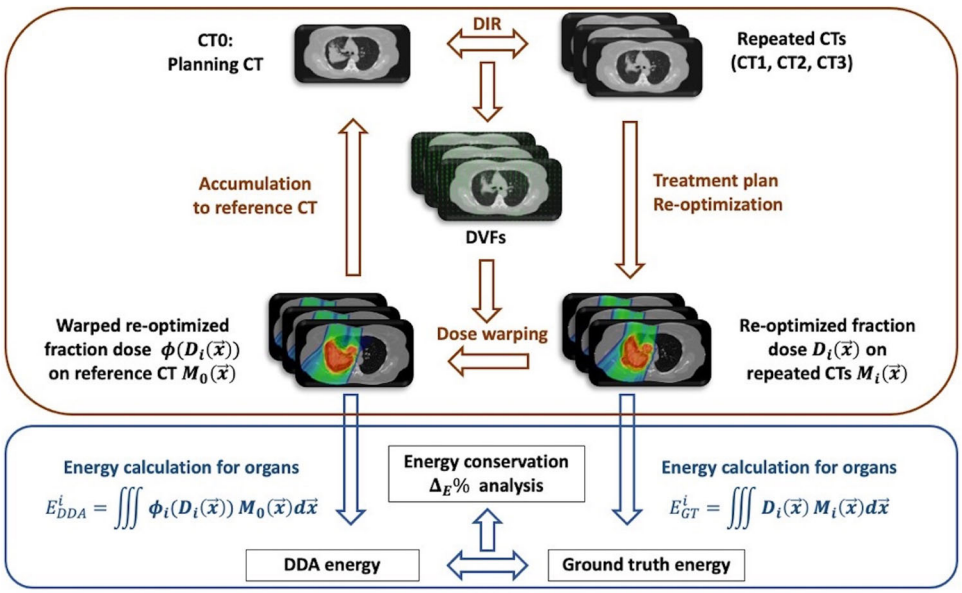

FIGURE 1 Workflow for deformable dose accumulation (brown box) and the proposed energy conservation-based validation (blue box)

variation also require extra caution for DDA.[5,6,14,15,18,20] Zhong et al. presented a conceptual study with spheres with changing masses to validate the potential problem with energy conservation (EC) for dose accumulation for tumors undergoing such mass changes.[20] This conceptual example study provides the foundation for our work, in which the validation was conducted for realistic patient cases, to the best of our knowledge, this was done for the first time. In this paper, we presented the investigation on the DDA uncertainty in the context of mass/volume changes and validated the clinical usefulness of EC based on the work by Zhong et al.[20] for patient-specific QA of DDA. Of note, this work assumes that the energy of two representations of the same dose should be conserved. The associated controversy on such an assumption will be described in the discussion.

Firstly, the principles and mathematics of EC for DDA are introduced. Then, the EC-based criterion is applied to the accumulated dose distributions for selected non-small cell lung cancer cases (NSCLC). A variety of treatment modalities, each including non-adaptive and adaptive scenarios, and multiple DIR methods are included in the investigation. Next, the scenarios where EC is violated are presented and analyzed. Finally, the impact of volume and mass changes on EC violation is studied.

2 | MATERIALS AND METHODS

2.1 | Patient cohort and treatment planning

In this study, five NSCLC cases and five different DIR methods (Velocity, Plastimatch Demon, Plastimatch Bspline, Mirada, Raystation Anaconda) were included and evaluated. Each patient has one planCT (reference anatomy) and three repeated CTs named CT1, CT2 and CT3 and acquired on days 2, 16, and 31 of the treatment. All CTs were acquired in deep inspiration breath-hold (DIBH) and the motion was monitored with the Real-time Position Management sytem (RPM, Varian Medical Systems Inc.). The complete acquisition scheme was published earlier.[21]

This work studies both non-adaptive and adaptive treatment scenarios. In the non-adaptive scenario, treatment plans were optimized for the planCT, followed by re-calculation on all repeated CTs. For this, repeated CTs are rigidly registered to the planCT and share the same structure set as the planCT. For the adaptive scenario, plans were instead re-optimized on the individual repeated CTs based on new targets and OARs delineated by a physician on each CT.

Five different types of treatment [intensity-modulated radiotherapy (IMRT), two intensity-modulated proton therapy (IMPT), and two combined proton-photon therapy (CPPT)] were studied individually to cover a broad range of treatment plans. The complete optimization framework, including the objectives, was recently published.[22] All dose distributions for one example patient are shown in Figure 2. Nine equispaced coplanar beams were used for the IMRT plan, while three patient-specific fields were used for IMPT Gantry. We also considered proton therapy with a fixed horizontal beamline (FHB) (IMPT FHB), where two-field IMPT is delivered at a gantry angle of 270° with two different couch angles. Moreover, two types of combined proton-photon treatment (CPPT) were also included. The CPPT Gantry plan simultaneously optimizes the IMPT Gantry with the IMRT fields, while the CPPT FHB is the optimal combination of the IMPT FHB and IMRT fields. The concept and potential of CPPT are described in other publications.[23–27] The purpose of examining various treatment modalities is to avoid limiting the investigations to a single treatment type.

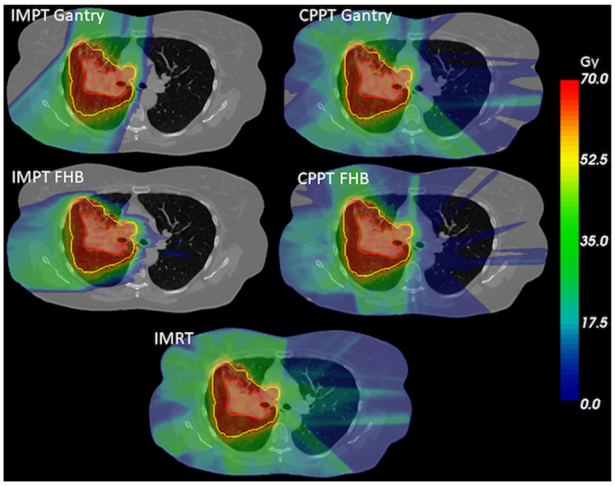

FIGURE 2 Dose distribution of the five treatment plans with contours of the GTV (red) and the PTV (yellow). CPPT FHB, combined proton-photon therapy with a fixed horizontal beamline; CPPT Gantry, gantry-based combined proton-photon therapy; IMPT FHB, intensity-modulated proton therapy with a fixed horizontal beamline; IMPT Gantry, intensity-modulated proton therapy; IMRT, intensity-modulated photon therapy

2.2 | Volume and mass variations

Previous work has demonstrated how EC can be violated under conditions of volume changes.[20] Such changes are also present in the five investigated cases here, mainly due to tumor regression relating to mass and volume changes during treatment.

Figure 3a illustrates the example volume variations, in which the volume V of the tumor (purple) is reduced to 50% while preserving density ρ, representing an ideal model for tumor shrinkage. In this case, intensity-based DIR algorithms try to match the contours of the two ROIs. If a uniform dose D is delivered to the target, the

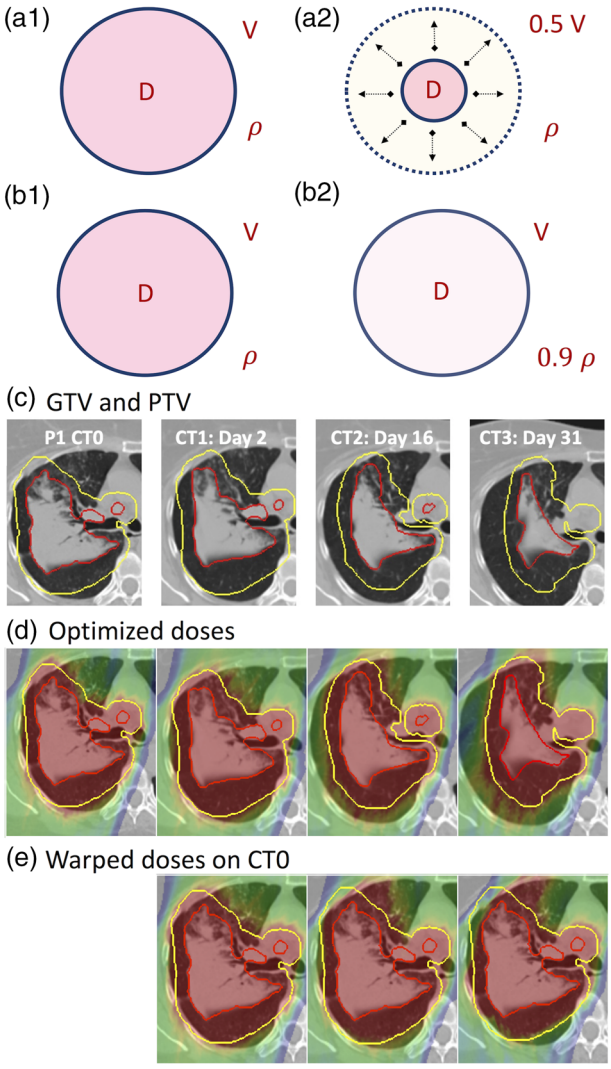

FIGURE 3. (a) Ideal model for ROI volume variation. (b) Ideal model for ROI density variation. (c) GTV (red) and PTV (yellow) variations in Patient 1 from planning day to treatment day 31. Similar variations were observed for the other patients and are shown in the supplement. (d) Optimized IMPT Gantry treatment plans for the respective CTs. (e) Warped doses on planning CT

energy on the repeated CTi is $0.5\rho VD$ (E = mD). However, in the warped representation, the energy is ρVD. This discrepancy leads to an overestimation of the total energy deposited to the tumor on day i when performing DDA.

In Figure 3b, the density of the target is reduced by 10% while the volume is kept constant. This is a model for mass variation introduced solely by density changes without any potential impact on the mass coming from volume changes. In this case, the boundaries are matched, and small (or nearly zero) DVF magnitudes are expected. The energy deposited on day i is $0.9\rho VD$. On the other hand, in the warped representation, the energy is ρVD. This leads again to an overestimation of the total energy delivered in DDA. One should notice that in real cases, density variation and volume variation are usually associated. As such, the total mass variation is a combined effect of both.

In Figure 3c, a real example of mass and volume variations for Patient 1 is displayed. For the other patients the variations are shown in the Supplementary material Figure S-1. From the planning day to the treatment day 31, the volume of the GTV reduced from 233 cm^3 to 135 cm^3 (−42.1%) and the mass reduced from 203 to 113 g (−44.3%). The mass is calculated by integrating all voxels in the GTV (or OARs) with densities calculated from a linear interpolation of the Hounsfield units (HU) to density look-up table used for the CT in the open-source treatment planning system matRad[28]:

$$M_{GTV} = \iiint \rho\left(\vec{x}\right)\, dV$$

For the PTV, the relative volume reduction was 28.1%, and the relative mass reduction was 38.6%. Such that for this patient, it is observed that the mass reduction for the PTV is around 10% larger than its volume reduction while for the GTV this difference is only around 2%. This can be explained by the specific anatomical situation, where lower density lung tissue is surrounding the tumor. Additionally, the ratio of the size between the GTV, with generally high-density tissue, and the PTV, which already includes lower density tissue, is of importance. The mass and volume changes for the GTV and PTV are summarized in the Supplement (Table S-1).

As described above, we studied both adaptive and non-adaptive treatment plans. The reason for this is to separate effects of density and volume variations. In adaptive plans, volume and density change are reflected in their combined effects on ROI mass. In contrast, in non-adaptive plans, since the shape and volume of the ROIs are kept constant, density variations are the only causes of ROI mass changes. As such, we can independently analyze its effect on EC.

2.3 | Energy conservation based DDA validation workflow

For any given repeated CTi, the ground truth (GT) total energy deposited to an ROI can be calculated by an integral over its volume:

$$E^i_{GT} = \iiint D_i\left(\vec{x}\right)\, M_i\left(\vec{x}\right) d\vec{x}$$

Here, the D_i and M_i represent the dose and mass distribution for CTi respectively. In DDA, however, the fraction doses are warped to a reference anatomy, which is usually the planning CT with mass distribution M_0. Thus, one can formulate the total energy in the new warped representation:

$$E^i_{DDA} = \iiint \phi_i(D_i\left(\vec{x}\right))\, M_0\left(\vec{x}\right) d\vec{x}$$

The mass distribution is then fixed to the reference anatomy M_0, while $\phi_i(D_i(\vec{x}))$ stands for the warped dose distribution of fraction i. ϕ_i is the transformation DVF generated by a DIR algorithm. $D_i(\vec{x})$ and $\phi_i(D_i(\vec{x}))$ are the two representations of the fraction doses on different anatomies.

The total energy deposited is a physical quantity determined by the interactions of photons/protons with the matter in the patient's body. On each treatment day, once the treatment is completed, the delivered protons/photons, their interactions with the matter, and consequently, the energy deposited in the patient become an unknown but irrevocable physical fact. In this work, we assume energy is conserved for any representation of the delivered dose in fraction i. This means that if the total energy, for example 10 J, is deposited in the PTV on a specific treatment day, then any representation of this dose should conserve this 10 J. However, intensity- and contour-based DIRs and corresponding DVF-based DDA, in principle do not guarantee this conservation, which might make the accumulation results under the assumption of EC in specific cases questionable.

In this study, the factor $\Delta_E\%$ is defined to quantify the extent to which EC is violated. For treatment with n repeated CTs and adaptations, the main quantities under consideration are defined in the following way:

$$E_{GT} = \sum_{i=0}^{n} E^i_{GT} = \sum_{i=0}^{n} \iiint D_i(\vec{x})\, M_i(\vec{x})\, d\vec{x}$$

$$E_{DDA} = \sum_{i=0}^{n} E^i_{DDA} = \sum_{i=0}^{n} \iiint \phi_i(D_i(\vec{x}))M_0(\vec{x})\, d\vec{x}$$

$$\Delta^i_E\% := 1 - \frac{E^i_{DDA}}{E^i_{GT}}$$

$$\Delta_E\% := 1 - \frac{E_{DDA}}{E_{GT}}$$

where E_{GT} and E_{DDA} represent the cumulative ground truth energy, and the DDA calculated energy. Positive $\Delta_E\%$ implies under-estimations of the total delivered energy, while negative $\Delta_E\%$ indicates over-estimations. For each repeated CT i and the respective re-optimized plan, a CT-specific EC analysis has been calculated with $\Delta^i_E\%$.

Based on the principle of EC above, we formalized a validation workflow for DDA shown in Figure 1 (blue box). In the validation process, the energies of the targets and OARs are calculated for the re-optimized dose distributions on the repeated CT and the warped fraction doses on the reference CT. Under our assumption, these two dose distributions are different representations of the same physical energy situation, such that the total energy deposited to a ROI for one fraction should be conserved for any representation of this dose distribution indicated by $\Delta^i_E\%$ value close to zero.

3 | RESULTS

In Figure 4, the E^i_{GT}(solid) and E^i_{DDA}(dashed) deposited to ROIs of Patient 1, this is the patient with the largest anatomical changes, are shown for the CPPT Gantry treatment plan. Results for all patients, treatment plans, and ROIs are plotted in the Supplementary material (Figure S-2 to S-5). For the other treatment plans, the results are very similar. Firstly, for the PTV and GTV, the ground truth energy E^i_{GT} decreases due to tumor shrinkage. On the other side, for the DDAs with five different DIR algorithms, the E^i_{DDA} stays close to the planning day even when significant regression existed, leading to a systematic overestimation with Δ^i_E reaching −78% for GTV and −52% for PTV on CT3 (day 31). As discussed above, the GTVs mass and volume reduction showed to be larger than for the PTV for this patient, additionally, due to the ratio between the GTV and PTV size, the PTV showed a smaller relative volume reduction. As a result, in the accumulated dose distribution, Δ_E ranges from −25.0% to −25.3% for GTV and −22.1% to −22.5% for PTV. The accumulation performed here represents a simplified situation, in which CT0-CT3 are considered as 4 fractions. Adding the GT energies and comparing it to the DDA values gives a simplified accumulated result, instead of only a fraction-wise. Another option would be to interpolate the data for the days with no data. One possibility would be to use a linear interpolation between the day 2 and day 16 for the first 15 treatment days, then a linear interpolation of the day 16 to day 31 data for the next 15 treatment days and then for the last 5 treatment days the value of day 31. These accumulation results averaged over the treatment modalities and DIR methods leads to a Δ_E of −40.9 ± 0.1% for the GTV and −32.1 ± 0.3% for the PTV. Looking at the OAR results, for the heart and spinal cord, E_{DDA} results were close to E_{GT} with Δ^i_E being randomly distributed within ±10%.

In general, strong EC violations were mainly found for targets (GTV and PTV). The smallest violation is seen for Patient 2 and 5, which show the smallest anatomical changes. For most OARs, EC violations were lower and tend to be random. In addition, for both targets and OARs, the discrepancy between five different DDAs regarding deposited energy was limited. These results are consistent across all the different treatment plan types and patients.

To investigate the relation between EC violation and volume/mass variation, Bayesian linear regressions (BLR) was performed. In Figure 5, BLR comparing Δ^i_E and relative mass variation, including data from all five patients and five treatment types, is shown. Δ^i_E values were calculated for one example DDA result (DIR: Velocity).

As seen above, the values for the different DIR methods are very similar. Firstly, in GTV, EC was violated in DDA, and we observed that the extent of EC violation was moderately linearly correlated with volume variation

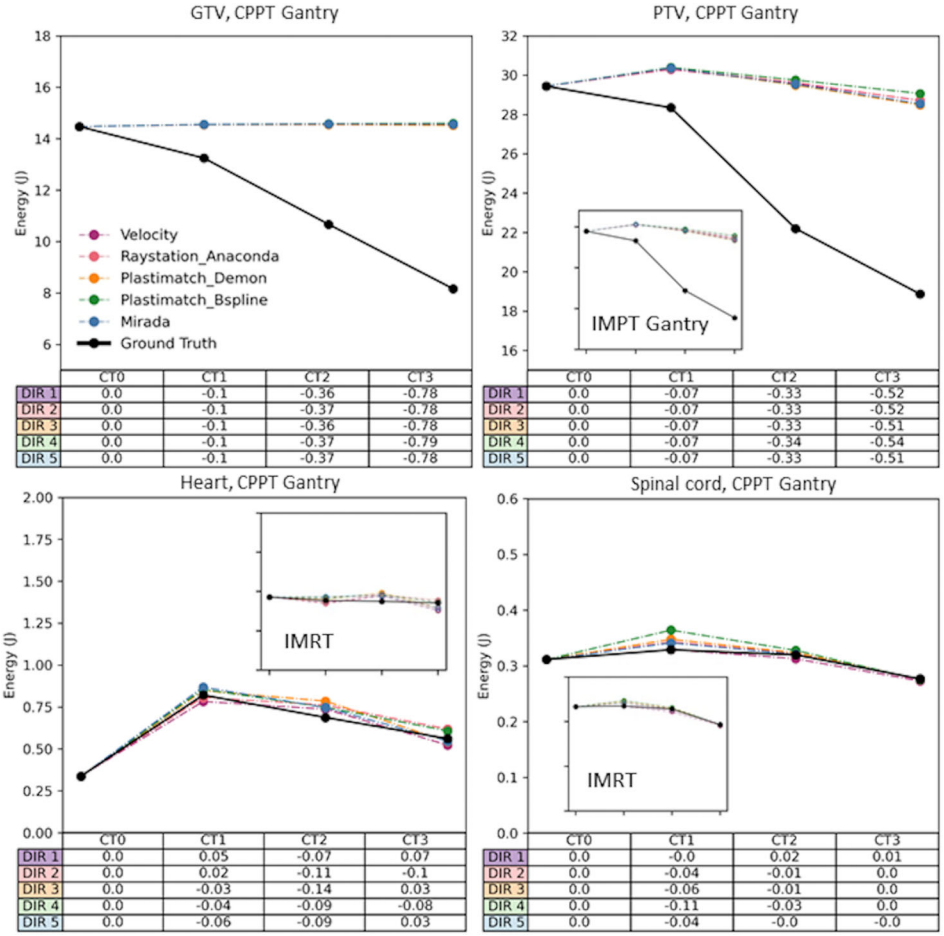

	CT0	CT1	CT2	CT3
DIR 1	0.0	-0.1	-0.36	-0.78
DIR 2	0.0	-0.1	-0.37	-0.78
DIR 3	0.0	-0.1	-0.36	-0.78
DIR 4	0.0	-0.1	-0.37	-0.79
DIR 5	0.0	-0.1	-0.37	-0.78

	CT0	CT1	CT2	CT3
DIR 1	0.0	-0.07	-0.33	-0.52
DIR 2	0.0	-0.07	-0.33	-0.52
DIR 3	0.0	-0.07	-0.33	-0.51
DIR 4	0.0	-0.07	-0.34	-0.54
DIR 5	0.0	-0.07	-0.33	-0.51

	CT0	CT1	CT2	CT3
DIR 1	0.0	0.05	-0.07	0.07
DIR 2	0.0	0.02	-0.11	-0.1
DIR 3	0.0	-0.03	-0.14	0.03
DIR 4	0.0	-0.04	-0.09	-0.08
DIR 5	0.0	-0.06	-0.09	0.03

	CT0	CT1	CT2	CT3
DIR 1	0.0	-0.0	0.02	0.01
DIR 2	0.0	-0.04	-0.01	0.0
DIR 3	0.0	-0.06	-0.01	0.0
DIR 4	0.0	-0.11	-0.03	0.0
DIR 5	0.0	-0.04	-0.0	-0.0

FIGURE 4 E^i_{GT} (J) (black) and E^i_{DDA} (J) (colored) for four ROIs of Patient 1 plotted for the planning CT (CT0) and three repeated CTs (I = 1,2,3). Five DIRs are used for DDA, represented by different colors (DIR 1 = Velocity, DIR 2 = Raystation Anaconda, DIR 3 = Plastimatch Demon, DIR 4 = Plastimatch Bspline, DIR 5 = Mirada). The Δ^i_E values for each CT are listed in the table. Next to CPPT Gantry, additional examples of other treatment plans are given to illustrate the very small differences. The complete results can be found in the supplementary material

($R^2 = 0.553$) as shown in Figure 5 (a-1). The relative total mass variation is a combined effect of both volume and density change, and as shown in Figure 5 (a-2), we observed regression results with $R^2 = 0.959$. Similar results were found for the PTV shown in Figure 5 (b-1, b-2), with $R^2 = 0.694$ and $R^2 = 0.977$ for relative volume and mass variation. In Figure 5 (c-1, c-2), BLR was implemented for the ipsilateral part of the lung. We observed limited volume/mass variation in this OAR with weak EC violation. The data points were centered close to the origin with the linear fitting with $R^2 = 0.363$ and 0.306 for relative volume and mass variation. For other OARs, we noticed some outliers. These outliers came from organs with very low doses/energy, such as the heart and spinal cord in IMPT. In the extreme case, we found some ROIs with $\Delta^i_E < -1000\%$, but the absolute energy change was below 0.1J. These points were therefore omitted from the regression.

For non-adaptive plans, similar EC violations were observed for the GTV and PTV, as shown in Figure 5 (a-3) and (b-3). Due to the constant structures used in the non-adaptive scenario, density changes were the only cause of mass variation and the R^2 values for the linear regression of GTV, PTV, and ipsilateral lung were 0.980, 0.988, and 0.612. For both adaptive and non-adaptive plans, the BLR results for PTV and GTV are plotted in the supplementary material for the five treatment plan types separately. Scatter plots have also been calculated for all OARs.

In general, it is observed that the volume variation has a lower correlation to the EC violation than the mass variations. Of note, a variation in volume is also correlated to a variation in mass. In the case of the adaptive plans, the relative mass variation is a combination of density changes and the change of the mass due to a variation in the volume. It is observed that the correlation to EC violation is higher for the mass variation. With the non-adaptive plans, it is possible to reduce to mass changes due to density changes, as the volumes are kept constant. In this case, the bands in the BLR are the

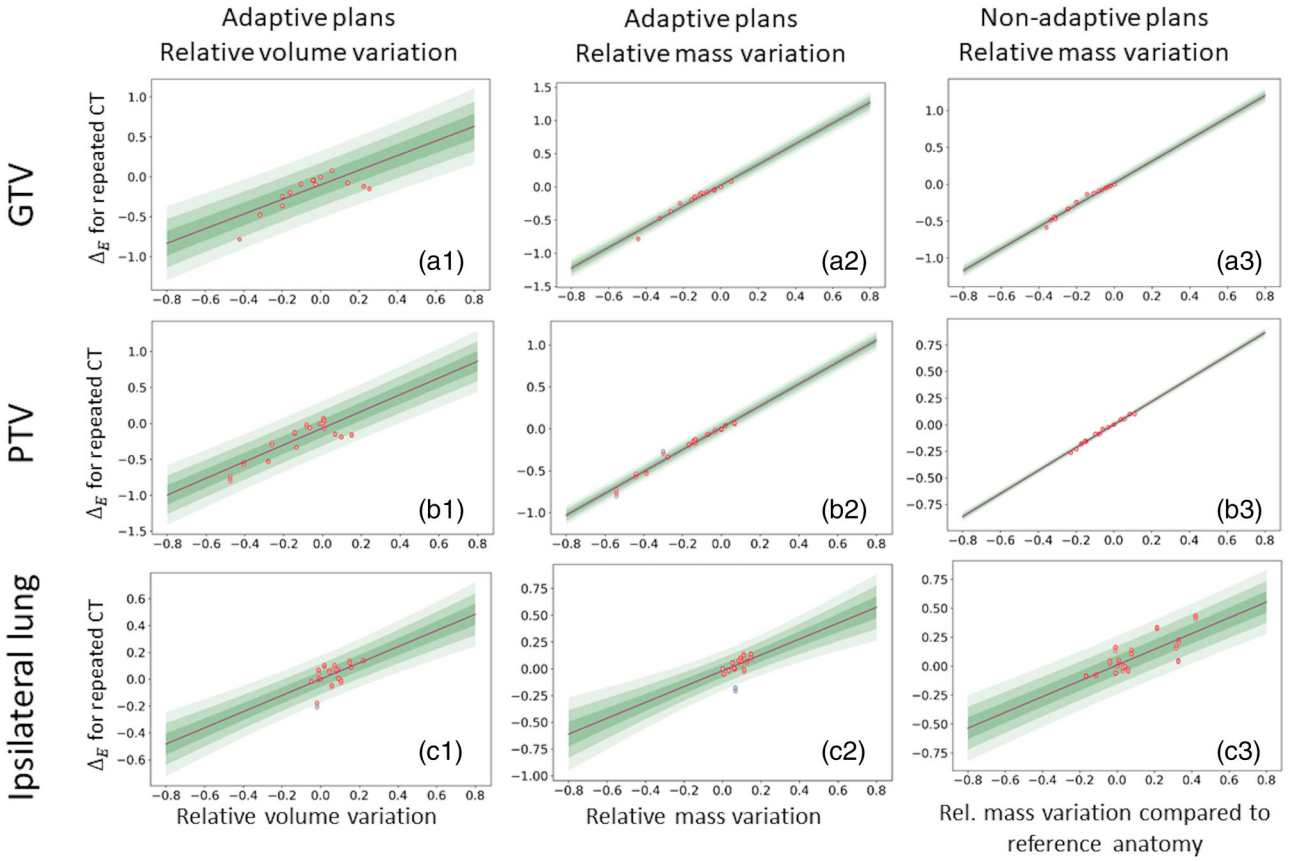

FIGURE 5 (a) GTV, (b) PTV, (c) ipsilateral lung. Column 1: Bayesian linear regression (BLR) for Δ_E^i of adaptive plans and relative volume variation. Column 2: BLR for Δ_E^i of adaptive plans and relative mass variation. Column 3: BLR for Δ_E^i of non-adaptive plans and relative mass variation. Mean prediction colored in purple and green bands mean 1 σ, 2 σ, 3 σ confidence intervals. Data points within/outside 3 œ are colored in red/blue

smallest and the correlation is the highest. Which indicates that the mass variations due to density changes are the main driver for the EC violation.

4 | DISCUSSION

The investigation of EC violation for DDA in mass/volume changing NSCLC cases showed multiple interesting findings. However, before discussing those findings, we want to emphasize again that this work is based on the assumption that energy needs to be conserved. Previous work has led to an active discussion of the adequacy of this assumption.[20,29,30] To summarize the main points of the discussion. The two positions are mainly discussing if the energy needs to be conserved, as the mass is changing over time. On one hand, proponents argue that the energy does not need to be conserved, as with the "lost" mass also part of the energy is lost.[29] Conversely, others contend that dose summing requires bringing doses from different time points, such as T1 and T2, to a common geometry, such as the planning CT at T1, which represents the initial state in which the mass existed in its entirety.[30] To the best of our knowledge there is still no consensus in the community. Nevertheless, lately, the medical image registration special interest group (MIRSIG) of the Australasian College of Physical Scientists & Engineers in Medicine also stated in their position paper on the use of image registration algorithms in radiotherapy that the violation of EC in non-mass preserving DIRs needs to be at least validated and investigated.[18] Therefore, we believe the assumption is reasonable and its consequences should be investigated.

A first finding concerns the dependency on the choice of the DIR algorithm and the treatment modality. From Figure 4 and the Figures in the supplementary material, the discrepancies between different DIRs have been found to be small, which means DIR ambiguities are not crucial in the EC analysis. This differs from the findings in studies in which the investigation focused on the dose level, where differences between DIR methods can lead to substantial differences in the warped dose.[10,16] In addition, in terms of deposited energy and EC in each ROI, the results of five different treatment plan types were almost the same despite their dissimilar dose

distributions outside of the target, which suggests that the characteristics of the ROIs and their changes are the major causes of EC violations.

Secondly, we observed substantial EC violations for PTVs and GTVs with a 20–30% total energy overestimation in the simplified accumulation case explained above. The BLR results showed that the extent of EC violation is linearly correlated to the ROI's relative volume/mass variation. Therefore, based on the EC criterion, DDA should indeed be used with caution in ROIs with considerable volume/mass variations.[14] However, previous research on EC remained theoretical. In this work, we implemented an EC validation of DDA and found EC violations in five NSCLC cases. This study could be extended in the future to other situations or indications impacted by substantial anatomical changes, such as for tumors in the abdominal or pelvic regions or for head and neck cancer cases. These investigations could evaluate the impact of different breath-holding/free-breathing situations, varying fullness of the stomach or bladder, or weight loss in the head and neck region. Furthermore, it would be important in the future to extend the investigations to a dataset including more time points to get a more accurate estimation on the EC violations.

The impact of volume and density variation on the EC in our work emphasizes the need for extended discussions and awareness on this topic in the community. For example, in Figure 3c, 28.0% of the PTV disappeared from CT0 to CT3. If the target volume is adapted, the effect of the CT3 fraction represented on CT0 is equivalent to a boosting dose to the remaining 72.0% volume. However, after the DDA, the dose will be warped to the initial full-size target volume, which does not match what was delivered and leads to the observed EC violation. On the other hand, if one assumes that the same initial PTV region should be treated because of the potential microscopic spread of the tumor,[31] then the density in this region still changes. In Figure 3c, the mean density of the PTV was decreased by 19.8% from CT0 to CT3. In DIR-based DDA, the dose will be mapped directly from low-density PTV in the repeated CT to the high-density PTV in the reference anatomy. This also leads to EC violations, and furthermore, also partly dilutes the actual delivery. One possible solution for the volume changes could be volume-preserving registration methods, such as the hybrid finite element method (FEM) based model.[32] These methods previously showed better performance than traditional DIR regarding volume preservation and EC. However, these methods are currently not widely available or used compared to intensity-based DIRs. For the density changes, a re-scaling of the dose might be an idea to consider in the future. For example, in Figure 3 (b-1, b-2), the mean density of the target was reduced to 90% in CT i. Therefore, for a better representation of the dose to be accumulated on the reference CT, the dose D should perhaps be adjusted to 90%D. Such consideration might lead to more accurate clinical outcome evaluation, such as tumor control, normal tissue complications, and dose-volume effects, as the adjustment of the upstream dose accumulation workflow influences the downstream clinical models. In light of these possible improvements, it is necessary for the radiotherapy community to further investigate and discuss on DDA processes.

5 | CONCLUSION

This study performed an investigation of the energy conservation problem of DDA in the context of mass changes on actual patient data. More specifically, it was shown that DDA with traditional intensity-based DIR violates energy conservation for regions with high mass/volume variation in lung cancer cases and that the extent of EC violation is linearly correlated to the relative mass/volume change. The proposed patient-specific EC validation can be a helpful validation tool for DDA.

ACKNOWLEDGMENTS

The Swiss Cancer Research Foundation (KFS-4528-08-2018) and Krebsliga Schweiz Research Grant (KFS-4517-08-2018) funded this work.

Open access funding provided by ETH-Bereich Forschungsanstalten.

CONFLICT OF INTEREST STATEMENT

The authors have no conflicts to disclose.

DATA AVAILABILITY STATEMENT

Due to the medical nature of the research, supporting data is not available.

REFERENCES

1. Glide-Hurst CK, Lee P, Yock AD, et al. Adaptive radiation therapy (ART) strategies and technical considerations: a state of the ART review from NRG Oncology. *Int J Radiat Oncol Biol Phys*. 2021;109:1054-1075. doi: 10.1016/j.ijrobp.2020.10.021
2. Bertholet J, Anastasi G, Noble D, et al. Patterns of practice for adaptive and real-time radiation therapy (POP-ART RT) part II: offline and online plan adaption for interfractional changes. *Radiother Oncol*. 2020;153:88-96. doi: 10.1016/j.radonc.2020.06.017
3. Castelli J, Simon A, Lafond C, et al. Adaptive radiotherapy for head and neck cancer. *Acta Oncol (Madr)*. 2018;57:1284-1292. doi: 10.1080/0284186X.2018.1505053
4. Ghilezan M, Yan D, Martinez A. Adaptive radiation therapy for prostate cancer. *Semin Radiat Oncol*. 2010;20:130-137. doi: 10.1016/j.semradonc.2009.11.007
5. Piperdi H, Portal D, Neibart SS, Yue NJ, Jabbour SK, Reyhan M. Adaptive radiation therapy in the treatment of lung cancer: an overview of the current state of the field. *Front Oncol*. 2021;11:1-12. doi: 10.3389/fonc.2021.770382
6. Oh S, Kim S. Deformable image registration in radiation therapy. *Radiat Oncol J*. 2017;35:101–111. https://doi.org/10.3857/roj.2017.00325
7. Fischer B, Modersitzki J. Ill-posed medicine - An introduction to image registration. *Inverse Probl*. 2008;24. https://doi.org/10.1088/0266-5611/24/3/034008

8. Zhang Y, Knopf A, Tanner C, Boye D, Lomax AJ. Deformable motion reconstruction for scanned proton beam therapy using online x-ray imaging. *Phys Med Biol*. 2013;58:8621–8645. https://doi.org/10.1088/0031-9155/58/24/8621
9. Ribeiro CO, Knopf A, Langendijk JA, Weber DC, Lomax AJ, Zhang Y. Assessment of dosimetric errors induced by deformable image registration methods in 4D pencil beam scanned proton treatment planning for liver tumours. *Radiother Oncol*. 2018;128:174–181. https://doi.org/10.1016/j.radonc.2018.03.001
10. Nenoff L, Ribeiro CO, Matter M, et al. Deformable image registration uncertainty for inter-fractional dose accumulation of lung cancer proton therapy. *Radiother Oncol*. 2020;0. https://doi.org/10.1016/j.radonc.2020.04.046
11. Hub M, Thieke C, Kessler ML, Karger CP. A stochastic approach to estimate the uncertainty of dose mapping caused by uncertainties in b-spline registration. *Med Phys*. 2012;39:2186–2192. https://doi.org/10.1118/1.3697524
12. Brock KK, Mutic S, McNutt TR, Li H, Kessler ML. Use of image registration and fusion algorithms and techniques in radiotherapy: Report of the AAPM Radiation Therapy Committee Task Group No. 132: Report. *Med Phys*. 2017;44:e43–e76. https://doi.org/10.1002/mp.12256
13. Jaffray DA, Lindsay PE, Brock KK, Deasy JO, Tomé WA. Accurate accumulation of dose for improved understanding of radiation effects in normal tissue. *Int J Radiat Oncol Biol Phys*. 2010;76:135–139. https://doi.org/10.1016/j.ijrobp.2009.06.093
14. Chetty IJ, Rosu-Bubulac M. Deformable registration for dose accumulation. *Semin Radiat Oncol*. 2019;29:198–208. https://doi.org/10.1016/j.semradonc.2019.02.002
15. Schultheiss TE, Tomé WA, Orton CG. It is not appropriate to "deform" dose along with deformable image registration in adaptive radiotherapy. *Med Phys*. 2012;39:6531–6533. https://doi.org/10.1118/1.4722968
16. Amstutz F, Nenoff L, Albertini F, Ribeiro CO, Knopf A-C, Unkelbach J, et al. An approach for estimating dosimetric uncertainties in deformable dose accumulation in pencil beam scanning proton therapy for lung cancer. *Phys Med Biol*. 2021;66:105007. https://doi.org/10.1088/1361-6560/abf8f5
17. Brock KK, Mutic S, McNutt TR, Li H, Kessler ML. Use of image registration and fusion algorithms and techniques in radiotherapy: report of the AAPM Radiation Therapy Committee Task Group No. 132. *Med Phys*. 2017;44:e43–e76. https://doi.org/10.1002/mp.12256
18. Lowther N, Louwe R, Yuen J, Hardcastle N, Yeo A, Jameson M. MIRSIG position paper: the use of image registration and fusion algorithms in radiotherapy. *Phys Eng Sci Med*. 2022;45:421–428. https://doi.org/10.1007/s13246-022-01125-3
19. Varadhan R, Hui SK. Applicability and limits of dose warping: are there islands of deformation that fail to depict dose painting? *Int J Radiat Oncol*. 2014;90:S861. https://doi.org/10.1016/j.ijrobp.2014.05.2463
20. Zhong H, Chetty IJ. Caution must be exercised when performing deformable dose accumulation for tumors undergoing mass changes during fractionated radiation therapy. *Int J Radiat Oncol Biol Phys*. 2017;97:182–183. https://doi.org/10.1016/j.ijrobp.2016.09.012
21. Josipovic M, Persson GF, Håkansson K, et al. Deep inspiration breath hold radiotherapy for locally advanced lung cancer: comparison of different treatment techniques on target coverage, lung dose and treatment delivery time. *Acta Oncol (Madr)*. 2013;52:1582–1586. https://doi.org/10.3109/0284186X.2013.813644
22. Amstutz F, Fabiano S, Marc L, et al. Combined proton – photon therapy for non-small cell lung cancer. *Med Phys*. 2022:1–13. https://doi.org/10.1002/mp.15715
23. Unkelbach J, Bangert M, De Amorim Bernstein K, Andratschke N, Guckenberger M. Optimization of combined proton–photon treatments. *Radiother Oncol*. 2018;128:133–138. https://doi.org/10.1016/j.radonc.2017.12.031
24. Fabiano S, Balermpas P, Guckenberger M, Unkelbach J. Combined proton–photon treatments – a new approach to proton therapy without a gantry. *Radiother Oncol*. 2020;145:81–87. https://doi.org/10.1016/j.radonc.2019.12.013
25. Amstutz F, Fabiano S, Marc L, et al. Combined proton-photon therapy for non-small cell lung cancer. *Med Phys*. 2022;49(8):5374–5386. doi:10.1002/mp.15715
26. Marc L, Fabiano S, Wahl N, Linsenmeier C, Lomax AJ, Unkelbach J. Combined proton – photon treatment for breast cancer. *Phys Med Biol*. 2021;66(23):235002. doi:10.1088/1361-6560/ac36a3
27. Kueng R, Mueller S, Loebner HA, et al. TriB-RT: simultaneous optimization of photon, electron and proton beams. *Phys Med Biol*. 2021;66(4):045006. doi:10.1088/1361-6560/ab936f
28. Wieser HP, Cisternas E, Wahl N, et al. Development of the open-source dose calculation and optimization toolkit matRad. *Med Phys*. 2017;44:2556–2568. https://doi.org/10.1002/mp.12251
29. Hugo GD, Dial C, Siebers JV. In regard to Zhong and Chetty. *Int J Radiat Oncol Biol Phys*. 2017;99:1308–1310. https://doi.org/10.1016/j.ijrobp.2017.08.047
30. Zhong H, Chetty IJ. In reply to Hugo et al. *Int J Radiat Oncol Biol Phys*. 2017;99:1310. https://doi.org/10.1016/j.ijrobp.2017.08.049
31. Sonke JJ, Aznar M, Rasch C. Adaptive radiotherapy for anatomical changes. *Semin Radiat Oncol*. 2019;29:245–257. https://doi.org/10.1016/j.semradonc.2019.02.007
32. Zhong H, Chetty IJ. Adaptive radiotherapy for NSCLC patients: utilizing the principle of energy conservation to evaluate dose mapping operations. *Phys Med Biol*. 2017;62:4333–4345. https://doi.org/10.1088/1361-6560/aa54a5

SUPPORTING INFORMATION

Additional supporting information can be found online in the Supporting Information section at the end of this article.

How to cite this article: Wu X, Amstutz F, Weber DC, Unkelbach J, Lomax AJ, Zhang Y. Patient-specific quality assurance for deformable IMRT/IMPT dose accumulation: Proposition and validation of energy conservation based validation criterion. *Med Phys*. 2023;1-9. https://doi.org/10.1002/mp.16564